Article

Influence of Fluid Physical Properties on Ink-Jet Printability

Daehwan Jang, Dongjo Kim, and Jooho Moon

Langmuir, **2009**, 25 (5), 2629-2635• DOI: 10.1021/la900059m • Publication Date (Web): 05 February 2009

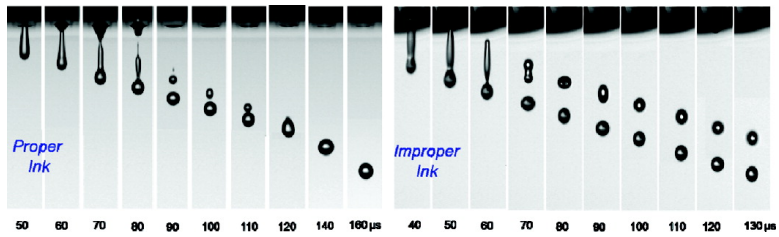

More About This Article

Additional resources and features associated with this article are available within the HTML version:

- Supporting Information
- Access to high resolution figures
- Links to articles and content related to this article
- Copyright permission to reproduce figures and/or text from this article

View the Full Text HTML

Influence of Fluid Physical Properties on Ink-Jet Printability

Daehwan Jang, Dongjo Kim, and Jooho Moon*

Department of Materials Science and Engineering, Yonsei University 134 Shinchon-dong Seodaemun-gu, Seoul 120-749, Korea

Received August 21, 2008

Ink-jet printing is a method for directly patterning and fabricating patterns without the need for masks. To achieve this, the fluids used as inks must have the capability of being stably and accurately printed by ink-jetting. We have investigated the inter-relationship between ink-jet printability and physical fluid properties by monitoring droplet formation dynamics. The printability of the fluids was determined using the inverse (Z) of the Ohnesorge number (Oh) which relates to the viscosity, surface tension, and density of the fluid. We have experimentally defined the printable range as $4 \leq Z \leq 14$ by considering characteristics such as single droplet formability, positional accuracy, and maximum allowable jetting frequency.

Introduction

Ink-jet printing is an emerging technology with many applications being explored beyond its image transfer capability, including microdispensing and materials assembly.[1−5] Recently it has been used to fabricate polymeric electroluminescent devices, controlled-release drug delivery devices, and refractive microlenses made of hybrid organic−inorganic materials.[2,6,7] The drop-on-demand (DOD) method is most commonly used for modern industrial applications. It deposits precise quantities of functional inks in the form of droplets on an arbitrary surface by applying a short pressure pulse through a nozzle which is typically 20−50 μm diameter.[8] The jetting operation mechanism involves the generation of pressure waves in a fluid-filled pathway behind an orifice. At the end of the orifice, the fluid meniscus is maintained by surface tension. A piezoelectrically induced pressure wave can propagate against the surface tension of the fluid, forming a small droplet which is ejected from the nozzle. Under suitable electrical conditions, the ejected fluid develops into a single droplet for quality ink-jetting.

However, appropriate functional ink materials are limited in availability. Inappropriate ink will lead to unstable ink-jetting in which long-lived filaments form, connecting the ejected droplet to the nozzle.[9] The length and lifetime of the filament influence the positional accuracy and resolution of the printing as well as the printability of the inks. Fluid dynamics involved in the ink-jet printing have been studied[10−13] and an atomistic understanding of ink-jet dynamics is recently emerging.[14,15] The important physical parameters of printing fluids are viscosity, density, and surface tension. These fluid properties influence the drop formation mechanism and subsequent drop size at a given voltage. Fromm obtained an approximate solution to the Navier−Stokes equations for the case of droplet ejection.[16] He used characteristic dimensionless numbers representing fluid physical properties. The Reynolds number (N_{Re}) is the ratio of inertial to viscous forces, and the Weber number (N_{We}) is a balance between inertial and capillary forces:[17]

$$N_{Re} = \frac{va\rho}{\eta} \tag{1}$$

and

$$N_{We} = \frac{v^2 a\rho}{\gamma} \tag{2}$$

where v, ρ, γ, and η are the average travel velocity, the density, surface tension, and viscosity of the fluid, and a is a characteristic dimension (the radius of the printing orifice). Another dimensionless number is the inverse (Z) of the Ohnesorge number (Oh), which is defined as the ratio between the Reynolds number and a square root of the Weber number, and is independent of fluid velocity:

$$Z = \frac{(a\rho\gamma)^{1/2}}{\eta} = \frac{N_{Re}}{(N_{We})^{1/2}} \tag{3}$$

On the basis of a numerical analysis using complete incompressible flow equations, Fromm predicted that stable drop formation in DOD systems is permitted only when $Z > 2$.[16] Later Reis and Derby determined that a printable fluid should have a Z value between 1 and 10. They explored the influence of fluid properties on ink-jet printing behavior using computational fluid dynamics that modeled the free-surface flow characteristics of drop formation in conjunction with a parallel experimental study. They found that the lower limit of Z is governed by the dissipation of the pressure pulse by fluid viscosity, and that the

* To whom correspondence should be addressed. E-mail: jmoon@yonsei.ac.kr. Tel.: +82-2-2123-2855. Fax: +82-2-365-5882.

(1) Derby, B.; Reis, N. *MRS Bull.* **2003**, *28*, 815–18.
(2) Gans, B.-J.; Duineveld, P. C.; Schubert, U. S. *Adv. Mater.* **2004**, *16*, 203–13.
(3) Jeong, S.; Woo, K.; Kim, D.; Lim, S.; Kim, J.; Shin, H.; Xia, Y.; Moon, J. *Adv. Funct. Mater.* **2008**, *18*, 679–86.
(4) Jeong, S.; Kim, D.; Moon, J. *J. Phys. Chem. C* **2008**, *14*, 5245–9.
(5) Kim, D.; Jeong, S.; Park, B.; Moon, J. *Appl. Phys. Lett.* **2006**, *89*, 264101 1–3.
(6) Xu, T.; Jin, J.; Gregory, C.; Hickman, J. J.; Boland, T. *Biomaterials* **2005**, *26*, 93–9.
(7) Tekin, E.; Smith, P. J.; Hoeppener, S.; Berg, A. M. J.; Susha, A. S.; Rogach, A. L.; Feldmann, J.; Shubert, U. S. *Adv. Funct. Mater.* **2007**, *17*, 23–8.
(8) Le, H. P. *J. Imaging Sci. Technol.* **1998**, *42*, 49–62.
(9) Gans, B.-J.; Kazancioglu, E.; Meyer, W.; Schubert, U. S. *Macromol. Rapid Commun.* **2004**, *25*, 292–6.
(10) Dong, H.; Carr, W. W.; Morris, J. F. *Phys. Fluids* **2006**, *18*, 072102–16.
(11) Xu, Q.; Basaran, O. A. *Phys. Fluids* **2007**, *19*, 102111–12.
(12) Zhang, X.; Basaran, O. A. *Phys. Fluids* **1995**, *7*, 1184–1203.
(13) Notz, P. K.; Chen, A. U.; Basaran, O. A. *Phys. Fluids* **2001**, *13*, 549–52.
(14) Li, F. I.; Leo, P. H.; Barnard, J. A. *J. Phys. Chem. C* **2008**, *112*, 14266–73.
(15) Lugli, F.; Zerbetto, F. *J. Phys. Chem. C* **2008**, *112*, 10616–10621.
(16) Fromm, J. E. *IBM J. Res. Dev.* **1984**, *28*, 322–33.
(17) Bergeron, V.; Bonn, D.; Martin, J. Y.; Vovelle, L. *Nature* **2000**, *405*, 772–5.

10.1021/la900059m CCC: $40.75
Published on Web 02/05/2009

Table 1. Summary of Physical Properties and Dimensionless Numbers for Each Fluid [a]

solvent type (volume fraction)	density (Kg/m^3)	viscosity (mPa·s)	surface tension (mN/m)	Reynolds number (N_{Re})	Weber number (N_{We})	inverse (Z) of Ohnesorge number (Oh)
ethylene glycol (0.15) + water (0.85)	1059	3.11	54.8	51.08	8.69	17.32
ethylene glycol (0.25) + ater (0.75)	1068	3.69	47.8	43.42	10.07	13.68
ethyl alcohol (0.75) + ethylene glycol (0.25)	866	4.83	28.9	26.89	13.47	7.32
ethylene glycol (0.5) + water (0.5)	1094	7.61	45.8	21.56	10.76	6.57
ethylene glycol (0.75) + water (0.25)	1106	12.3	45.6	13.49	10.91	4.08
glycerol (0.66) + Water (0.33)	1172	16.05	56.2	10.95	9.37	3.57
diethylene glycol (0.5) + water (0.5)	1111	22.0	41.4	7.58	12.08	2.17
diethylene glycol	1118	35.1	44.8	4.78	11.23	1.43

[a] Droplet diameter and its travel velocity are assumed to be 50 μm and 3 m/s, respectively.

upper limit is determined by the point at which a satellite forms instead of single droplet.[18]

In this study, we redefine the printable range of Z by in situ monitoring of droplet formation dynamics for various fluids having different Z values. We can determine the printable range by considering characteristics of printability such as single droplet formability, the minimum stand-off distance (i.e., the distance from the nozzle tip to the substrate), positional accuracy, and maximum allowable jetting frequency. These can be used to reduce the number of experiments needed to determine the optimal ink-jetting conditions for each fluid.

Experimental Section

To investigate drop formation dynamics during ink-jet printing, we set up an ink-jet printing system consisting of a nozzle, a jetting driver (pressure pulse generating system), a charge-coupled-device (CCD) camera, and a system computer. The ink-jet nozzle with an orifice diameter of 50 μm was manufactured by MicroFab Technologies, Inc. (Plano, TX). These employ a radial polarized lead zirconate titanate (PZT) type 5H tube actuator, with electrodes on the inner and outer cylindrical faces. This is rigidly bonded to a glass tube with an epoxy. The print head was mounted on a computer-controlled three-axis gantry system capable of movements accurate to $\pm$5 μm. In an ink-jet system, it is important to operate at proper pressure conditions for stable drop formation. To address this, a well-conditioned pressure waveform was kept constant. We used a bipolar waveform which consists of a succession of two square-wave (positive and negative) pulses. This waveform allowed a high voltage difference without applying too much high pulse amplitude. The dwell time was also set at 3 μs, and the echo time was set to be three times longer. The dwell and echo voltages were set at +25 and −25 V, respectively. Under a constant pressure pulse at the jetting frequency of 1 kHz, the various Z values caused each fluid to have a different drop filament formation and ejection behavior.

The CCD camera took snapshots of the drop formation dynamics with an interframe time of 1 μs. It was equipped with a strobe LED light to view individual droplets and to measure their sizes and travel velocities. The drop dynamics were captured by increasing the delay time of the camera in steps of 1 μs. Droplet images were taken at various delay intervals and showed the flight distance from the nozzle tip. The printing was carried out at a relative humidity of 40% at 25 °C.

Eight different fluids with physical properties characterized by Z values in the range of 1−17 were utilized.[19] The prepared fluids included a mixture of distilled water and ethylene glycol, a mixture of distilled water and diethylene glycol, a mixture of ethyl alcohol and ethylene glycol, a mixture of glycerol and distilled water, and pure diethylene glycol. Viscosity and surface tension were measured using a Peltier concentric-cylinder double-gap rheometer (AR2000ex, TA Instruments Inc., UK) and a tensiometer (DST30, SEO). The physical properties and dimensionless numbers for each fluid are summarized in Table 1.

Results and Discussion

Droplet formation behavior during piezoelectric DOD ink-jet printing is influenced by the system's response to an applied pressure stimulus on the fluid.[20,21] Drop ejection is the result of the superposition of consecutive acoustic waves that generate pressure pulses large enough to overcome viscous dissipation and the energy associated with forming a new surface. Reis et al. found that drop velocity and volume exhibit a linear relation with driving voltage, but show a more complicated and periodic behavior with changing frequency and pulse width (i.e., dwell time).[16] This periodic dependence is determined by the acoustic properties of the fluid-filled chamber in the piezoelectric droplet generator, which is a function of the fluid properties, print head design, and constituent materials. Hence, each individual fluid with different physical properties may have specific optimum printing conditions where the desired superposition of the acoustic pressure waves is achieved.

The fluid property that has an effect on the propagation and reflection of the acoustic pressure waves is acoustic velocity (c), represented by $c = (K/\rho)^{1/2}$ where K and ρ are the bulk modulus and density of the fluid, respectively. However, we studied the printability of various fluids under the same electrical driving condition because we used the bipolar waveform in which the second negative voltage could be used to cancel the residual acoustic oscillations that remain in the piezoelectric device after drop ejection. Our test liquids were particle-free Newtonian fluids with low viscosities and relatively similar densities and bulk moduli, which made the difference in the acoustic velocities small (within a range of 1480−1580 m/s). The droplet velocities of test fluids increased almost linearly with the increasing pulse width, in the range of 3−10 μs, under the bipolar waveform. These results were indicative of the absence of a periodic dependence at a low driving voltage of 25 V. Furthermore, we calculated the optimum pulse width (t_w), given by the time taken for an acoustic disturbance to travel from its origin near the center of the actuating chamber to its end and then back. The calculated t_w was in the range of 4−5 μs for our test fluids in a simple tubular actuated piezoelectric print head (MicroFab MJ-AT-01). Therefore, we were able to focus on the interrelationship between ink-jet printability and physical fluid properties by monitoring the droplet formation dynamics without the consideration of acoustic effects. Figure 1 shows a representative photo sequence of drop formation for fluids with Z values ranging from 2 to 17 at a constant driving voltage of 25 V.

The dynamics of fluid droplet formation as a function of the Z values are apparently different as physical properties of fluid. The inverse of the Ohnesorge numbers for the fluids shown in

(18) Reis, N.; Derby, B. *Mater. Res. Soc. Symp. Proc.* **2000**, *625*, 117–22.
(19) Son, T.; Teja, A. S. *J. Chem. Eng. Data* **2003**, *48*, 198–202.
(20) Dijksman, J. F. *J. Fluid Mech.* **1984**, *28*, 173–91.
(21) Antohe, B. V.; Wallace, D. B. *J. Imaging Sci. Technol.* **2002**, *46*, 409–14.

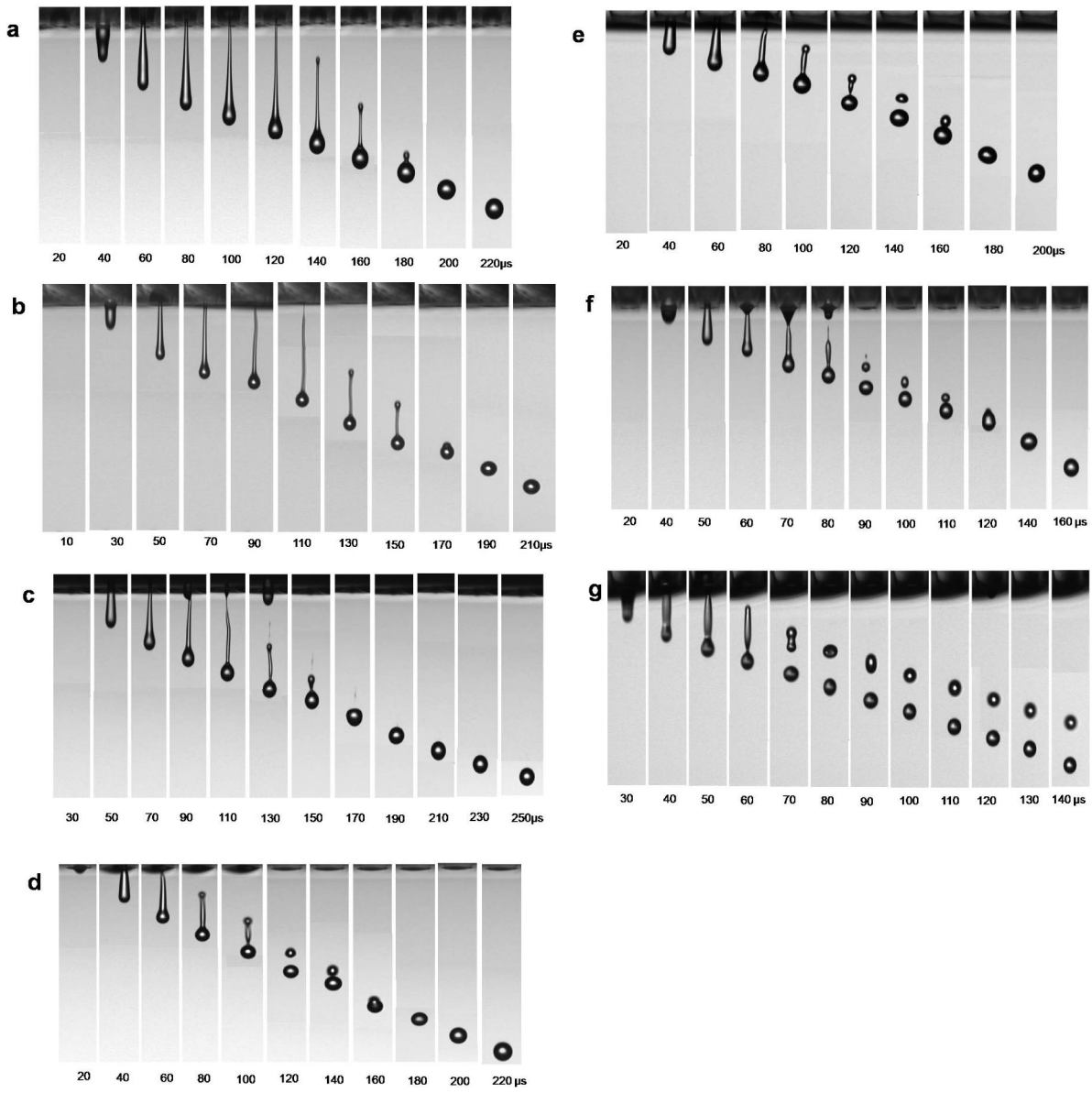

Figure 1. Representative photo sequence of drop formation for fluids with values of Z ranging from 2 to 17 at a constant driving voltage of 25 V: (a) $Z = 2.17$; (b) $Z = 3.57$; (c) $Z = 4.08$; (d) $Z = 6.57$; (e) $Z = 7.32$; (f) $Z = 13.68$; and (g) $Z = 17.32$.

Figure 1a,b,c,d,e,f,g are 2.17, 3.57, 4.08, 6.57, 7.32, 13.68, and 17.32, respectively. The pressure pulse pushed the fluid out of the nozzle tip and the meniscus bulged quickly until a filament with a round head formed at an elapsed time of 20−40 μs. The traveling velocity difference between the droplet head and the filament stretched the droplet filament until an elapsed time of about 60−120 μs. During the stretching of the fluid filament, the tail of the filament near the nozzle tip was continuously necking, forming a long fluid filament. The tail of the filament finally ruptured from the nozzle tip and recoiled back to the drop head to minimize surface area in the fluids with Z in the range of 2−4. The filament length shrank further and a single droplet eventually formed at an elapsed time of 160−200 μs (Figure 1a,b,c). On the other hand, for fluids with Z in the range of 6−13 (Figure 1d,e,f), the recoiling filament detached from the falling droplet, generating a primary droplet and a transient satellite, both of which merged together into a single droplet at an elapsed time of 140−180 μs. In contrast, for the fluid with a value of Z equal to 17.32, the satellite was unable to merge with the primary droplet even after 200 μs (Figure 1g).

As seen in the in situ monitoring, the droplet formation process involved the successive events of ejection and stretching of the fluid, necking, rupture, and recoil of the fluid, and formation and recombination of a single droplet and a satellite. For a quantitative analysis of droplet formation behavior, the positions of several representative points on the ejected fluid were plotted versus the elapsed time (Figure 2). In the earliest stage, the black colored dots represent the head trajectory of the fluid ejected from the nozzle, which became the tip of the primary droplet at a later stage. The red colored dots indicate the point at which the fluid ruptured from the nozzle, which represents the later tail trajectory of the fluid filament. The time at which the filament ruptured from the nozzle is defined as the rupture time. The moment at which the head and tail trajectories merged corresponds to the formation of a single droplet. This graphical description divides the jetting process into three distinct stages: filament elongation, filament recoiling, and single droplet formation. Figure 2 enables us to investigate jetting behavior as a function of Z.

For fluids with low Z values in the range of 2−4 (Figure 2a,b,c), a round protruding head formed on the filament at an

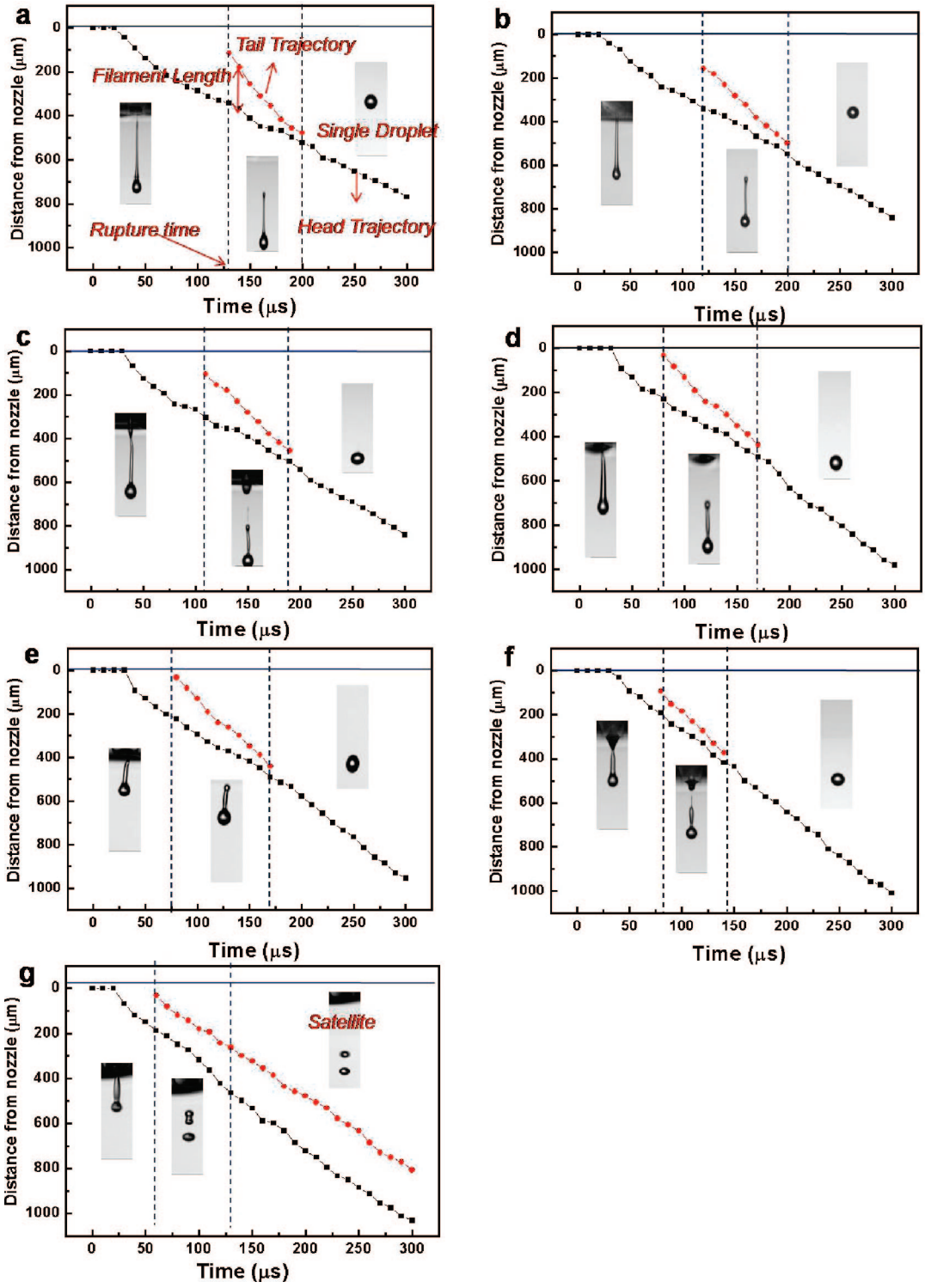

Figure 2. Representative trajectories of the ejected droplets as a function of the elapsed time for fluids with values of Z ranging from 2 to 17 at a constant driving voltage of 25 V: (a) $Z = 2.17$; (b) $Z = 3.57$; (c) $Z = 4.08$; (d) $Z = 6.57$; (e) $Z = 7.32$; (f) $Z = 13.68$; and (g) $Z = 17.32$.

elapsed time of about 50 μs, and the filament stretched until a time of about 120 μs. Filament rupture occurred at about 140 μs. In contrast, fluids with medium Z values in the range of 6−13, were subjected to faster filament elongation and earlier rupture as shown in Figure 2d,e,f. The fluid bulged to form a round filament head at a time of about 40 μs, and filament elongation occurred until about 60 μs. The bulge eventually ruptured at about 80 μs. Fluids with high Z values of above 14 experienced even more rapid filament elongation and rupture as shown in Figure 2g. The slope of the head trajectory represents the travel velocity of the falling droplet. Within a short travel distance of 1000 μm, we can ignore gravity-induced acceleration and assume that falling microdroplets with small masses travel at a constant velocity, even though the droplet size varies with the Z value. The travel velocity of the droplet increased with increasing Z values: 2.60 m/s when $Z = 2.17$, 2.85 m/s when $Z = 3.57$, 2.88 m/s when $Z = 4.08$, 3.4 m/s when $Z = 6.57$, 3.45 m/s when $Z = 7.32$, 3.63 m/s when $Z = 13.68$, and 3.66 m/s when $Z = 17.32$. In contrast, the retreating velocity of the tail (as determined by the slope of the tail trajectory) decreased with increasing Z value:

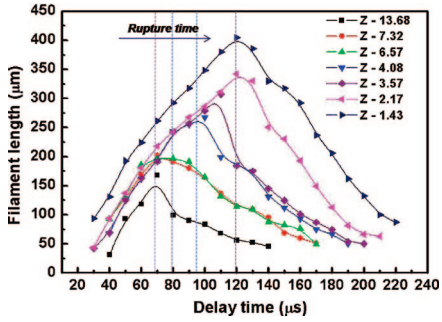

Figure 3. Filament length variation as a function of the delay time for fluids with varying *Z* values.

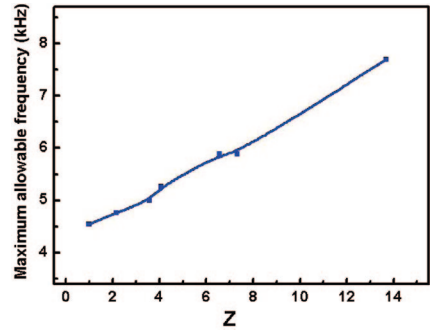

Figure 4. Maximum allowable frequency for quality ink-jet printing as a function of Z.

5.29 m/s when $Z = 2.17$, 4.46 m/s when $Z = 3.57$, 4.45 m/s when $Z = 4.08$, 4.38 m/s when $Z = 6.57$, 4.37 m/s when $Z = 7.32$, 4.30 m/s when $Z = 13.68$, and 3.16 m/s when $Z = 17.32$. These opposite tendencies caused the filament recoiling stage to occur within 70−90 μs, independent of the value of Z.

Jetting behavior dependence upon the Z values results from the influence of fluid properties on the ejection process, and the resulting travel velocity difference between the head and tail at the moment of filament rupture. After the ejected fluid ruptured from the nozzle, it became a free-flying filament. The travel velocity of the filament depends on the fluid viscosity and volume near the nozzle tip under a given pressure stimulus. The driving pressure applied to the fluid near the nozzle tip is viscously dissipated and consumed to form a new surface, while the remaining energy transforms into the kinetic energy of the ejected fluid. A higher fluid viscosity leads to more energy dissipated, resulting in a smaller available kinetic energy. Therefore, as the value of *Z* decreased, the travel velocity of the droplet head decreased due to the increased viscosity. The fluid volume near the nozzle tip, which determines the amount of viscous dissipation, also influences the travel velocity of the fluid. A viscous fluid forms a longer filament during printing, which narrows the filament neck at the nozzle tip. This reduces the fluid volume prior to rupture. The travel velocity of the tail increases with increased fluid viscosity. For fluids with low values of *Z*, in the range of 2−4, the relative tail velocity was fast enough to catch up to the droplet head, even at large separation distances. The tail merged with the head without a secondary rupture of the filament from the droplet. In the case of fluids with medium *Z* values, in the range of 6−13, a secondary rupture of the elongated filament from the falling droplet head occurred because of surface tension driven minimization of the surface area, but the tail velocity remained sufficiently fast to recombine with the primary droplet during the filament recoil stage. In contrast, fluids with high *Z* values, above 14, were easily ejected by the applied pressure without significant viscous dissipation. Large oscillatory kinetic energy and high surface tension tended to induce a secondary rupture of the filament which formed transient satellites. The resulting droplet fell with a relatively high travel velocity, so that the separated tail could not catch up with the droplet head. This generated a primary droplet and permanent satellites. This unstable jetting behavior means that fluids with values of *Z* above 14 are not printable fluids.

Single droplet formation occurred at 210 μs for $Z = 2.17$, 200 μs for $Z = 3.57$, 190 μs for $Z = 4.08$, 170 μs for $Z = 6.57$, 170 μs for $Z = 7.32$, and 130 μs for $Z = 13.68$. This indicates that fluids with higher *Z* values can form droplets at higher frequencies. Figure 3 also shows the filament length variation as a function of the delay time for fluids with varying *Z* values. As the *Z* values decreased, the droplet filament extended longer and its rupture time was delayed. The *Z* values for the fluids tested in this study decreased mainly because of increased viscosities, while having similar surface tensions regardless of *Z* values. A fluid with higher viscosity (i.e., lower *Z*) required a longer application of pressure for jetting due to significant viscous dissipation which caused longer filament formation and delayed droplet ejection.

Ink-jet printing speed is closely related to processing time and cost. Many existing ink-jet systems for image transfer purposes have firing frequencies of only 1−2 kHz. However, manufacturers have begun to demand frequencies of 10 kHz or higher.[25] The printing frequency is influenced by the print-head design as well as by fluid properties. For a given print-head, the inverse of the time required to form a single droplet can be considered as a maximum allowable printing frequency. Figure 4 shows the maximum allowable frequency for quality ink-jet printing as a function of *Z*. As *Z* increased from 1.4 to 13.68, the printing frequency increased linearly from 4.54 to 7.69 kHz under a constant driving voltage. It should be noted that any possible change in sound velocity with liquid compositions can cause an acoustic response difference in the piezoelectric device. This may alter the propagation speed of the acoustic pressure wave, even if the jetting was performed at the same driving voltage and pulse width. This effect leads to changes in both the droplet ejection speed and the time taken for single droplet formation. As mentioned previously, our fluids had relatively similar densities and bulk moduli, and the acoustic velocities were in the range of 1480 - 1580 m/s. It is likely that this small variation does not induce a significant change in the ejection time.

Ink-jetting is characterized by noncontact printing, so that the nozzle must be separated from the substrate during the print process. The distance between the nozzle and the substrate, that is, the stand-off distance, significantly influences the printing accuracy. Direct-writing of high-resolution features requires uniform droplet deposition. The flying distance, where the fluid ejected from the nozzle transforms into a single droplet, can define the minimum stand-off distance (MSD). Printing performed at a distance of less than the MSD results in the deposition of droplets having tails and satellites, degrading the printing resolution. Figure 5a shows the variation in minimum stand-off distance as a function of *Z*. As *Z* decreased from 13.68 to 4.08, the MSD increased linearly from 436 to 541 μm under a constant driving voltage, but soared to 650 μm when $Z < 4$. Ink-jet printing at longer MSDs leads to unstable and inaccurate deposition.

The total positioning accuracy during printing is influenced by several factors such as flight-bending of the droplet at the nozzle, deviations in flight velocity, the mechanical inaccuracy of the $x-y$ table, and the stand-off distance. The total patterning error (D) is given by the formula $D = (A^2 + B^2 + C^2)^{1/2}$, where A is the stand-off distance positioning error, B is the flight bending positioning error, and C is the mechanical positioning error.[26]

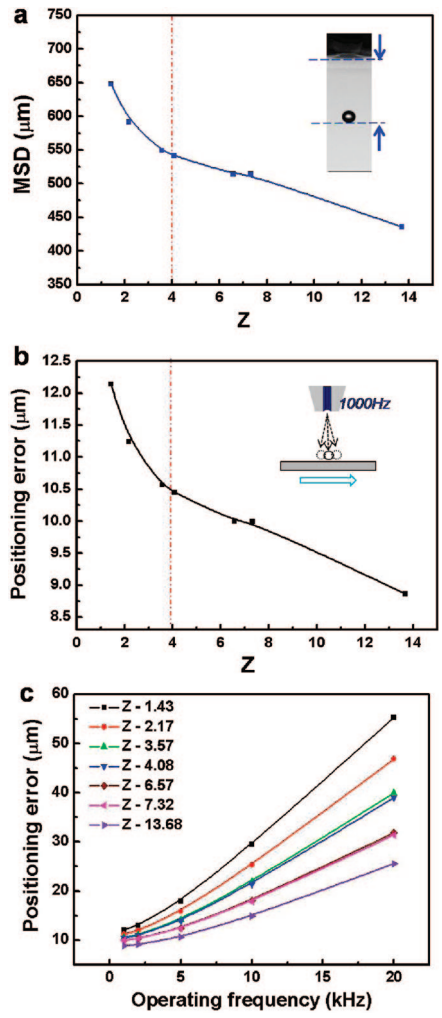

Figure 5. (a) Variation of the minimum stand-off distance (MSD) as a function of *Z*; (b) calculated positioning error as a function of *Z*; and (c) calculated positioning error as a function of the operating frequency.

The stand-off distance positioning error reflects the difference in flight times experienced by each droplet. The droplet should travel the stand-off distance after its ejection prior to landing on the substrate. Travel time varies depending on the stand-off distance under a given travel velocity. Within that time, the landing position deviates from the target as the $x-y$ stage moves, which is represented by *A*. The positioning error caused by flight bending (*B*) is also affected by the stand-off distance when the bending angle is fixed at $\pm 0.95°$. The mechanical positioning error (*C*) of recently developed $x-y$ moving tables is typically ± 5 μm. Then the total patterning error *D* under a constant applied driving voltage of 25 V, and a jetting frequency of 1 kHz can be calculated using the minimum stand-off distance. We observed that the positioning error became larger with decreasing *Z* values, similar to the dependence of the MSD as shown in Figure 5b: ± 12.1 μm for fluids with *Z* of 1.43, ± 11.2 μm for fluids with *Z* of 2.17, ± 10.5 μm for fluids with *Z* of 3.57, ± 10.6 μm for fluids with *Z* of 4.08, ± 10.0 μm for fluids with *Z* of 6.57, ± 9.9 μm for fluids with *Z* of 7.32, and ± 8.9 μm for fluids with *Z* of 13.58. It should be noted that the positioning error became significant as the operating frequency increased. Figure 5c shows the variation in positioning error as a function of the operating frequency. At a frequency of 10 kHz, the total patterning error was ± 29.5 μm for fluids with a *Z* of 1.43, ± 25.3 μm for fluids with a *Z* of 2.17, ± 21.9 μm for fluids with a *Z* of 3.57, ± 21.4 μm for fluids with a *Z* of 4.08, ± 18.1 μm for fluids with a *Z* of 6.57, ± 17.8 μm for fluids with a *Z* of 7.32, and ± 14.9 μm for fluids with a *Z* of 13.58.

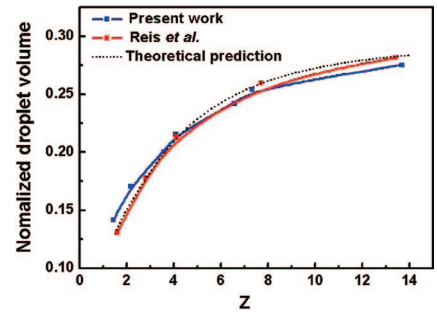

Figure 6. Variation of the normalized volume of a single droplet generated from a nozzle of 50 μm as a function of *Z* under the constant driving voltage of 25 V. Relevant previous works, theoretical prediction by Fromm[16] and the experimental result by Reis et al.,[22] are inserted for purposes of comparison.

These observations clearly demonstrate that fluid properties influence ink-jet printability. The test fluids included a pair of liquids with different densities, viscosities, and surface tensions; however, both fluids have similar *Z* numbers (i.e., liquids with *Z* values of 6.57 and 7.32; liquids with *Z* values of 3.57 and 4.08). A comparison of drop formation dynamics between these liquids confirms that the density, viscosity, and surface tension of each individual fluid interact with each other, and printability is determined by the inverse of the Ohnesorge number, not by the Reynolds number. Printing with fluids having $Z < 4$ led to longer times for single droplet generation, which in turn made the minimum stand-off distance larger and magnified the positioning errors. For this reason, fluids with *Z* values below 4 are considered to be inappropriate for high-resolution ink-jet printing. Figure 6 shows the normalized volume of a single droplet generated from a nozzle of 50 μm under constant pressure as a function of *Z*. The droplet volume is normalized by the volume displaced by the tubular actuator, which can be explicitly calculated from the mechanical and piezoelectric properties of the droplet generator assembly, that is,glass tube, epoxy, and PZT actuator.[22−24] The specific material properties and nozzle dimensions were provided by the manufacturer, and the calculations were performed assuming that the fluid and the glass tube have the same axial displacement. Our observation shows that droplet volume increases with increasing *Z* values, which follows a similar trend for a wide range of fluids, in accordance with Fromm's theoretical prediction and previous findings by Reis et al.[16,22] This picture represents a master curve relating fluid properties to drop volume for a given displacement of the current print-head.

Conclusions

We have investigated the inter-relationship between ink-jet printability and the print fluid's physical properties. By in situ monitoring of jetting dynamics using an image system with an interframe time of 1 μs, the droplet formation behavior was characterized in terms of the inverse of the Ohnesorge number which is related to the viscosity, surface tension, and density of the fluid. We have redefined the printable range as $4 \leq Z \leq 14$ by considering characteristics of printing such as single droplet

(22) Reis, N.; Ainsley, C.; Derby, B. *J. Appl. Phys.* **2005**, 094903 1–6.
(23) Reis, N.; Ainsley, C.; Derby, B. *J. Am. Ceram. Soc.* **2005**, *88*, 802–8.
(24) Bugdayci, N.; Bogy, D. B.; Talke, F. E. *IBM J. Res. Dev.* **1983**, *27*, 171–80.
(25) Creagh, L. T.; McDonald, M. *MRS Bull.* **2003**, *28*, 807–11.
(26) Shimoda, T.; Morii, K.; Seki, S.; Kiguchi, H. *MRS Bull.* **2003**, *28*, 821–7.

formability, the minimum stand-off distance, positional accuracy, and maximum allowable jetting frequency. Printing using a fluid with a low Z value (less than 4) resulted in droplet formation with a long-lived filament and a long time to single droplet generation. This degraded the positional accuracy and printing resolution. Fluids with high Z values (above 14) were also inappropriate for ink-jet printing because of their inability to form a single droplet. These low viscosity fluids had easy droplet ejection without significant viscous dissipation. Large oscillatory kinetic energy and high surface tension detached the retreating filament from the rapidly falling primary droplet, forming undesired satellites. A suitable ink-jet printing range will indicate whether or not a fluid can be stably and accurately printed by ink-jetting.

Acknowledgment. This work was supported by the Korea Science and Engineering Foundation (KOSEF) through the National Research Laboratory. The program was funded by the Ministry of Education, Science and Technology (No. R0A-2005-000-10011-0).

LA900059M